Contribution from the Department of Chemistry, Birkbeck College, University of London, London WC1E 7HX, U.K., Cancer Research Campaign Biomolecular Structures Research Group, Department of Biophysics, King's College, London WC2B 5RL, U.K., and Smith Kline & French Laboratories, Philadelphia, Pennsylvania 19101

Tertiary Phosphine Complexes of Gold(I) and Gold(III) with Imido Ligands: ^{1}H, ^{31}P, and ^{15}N NMR Spectroscopy, Antiinflammatory Activity, and X-ray Crystal Structure of (Phthalimido)(triethylphosphine)gold(I)

SUSAN J. BERNERS PRICE,† MICHAEL J. DiMARTINO,§ DAVID T. HILL,§ REIKO KURODA,‡ MUHAMMED A. MAZID,† and PETER J. SADLER*†

Received April 8, 1985

The preparation of a series of (imido)gold(I) tertiary phosphine complexes, $R_3PAu(NR')$ where the imido ligand ($R'N^-$) is phthalimide (ptm), diphenylhydantoin, saccharin, riboflavin or (tetrahydrosuccinimido)acenaphthenone, is described. A linear, two-coordinated structure was determined for $Et_3PAu(ptm)$, $AuC_{14}H_{19}NO_2P$, by X-ray crystallography: P–Au = 2.24 Å, Au–N = 2.05 Å, orthorhombic, space group $Pc2_1n$, a = 11.004 (1) Å, b = 11.023 (1) Å, c = 12.687 (2) Å, Z = 4. The L_{III} X-ray absorption spectra of the complexes all exhibited distinct edge features. Evidence that the riboflavin complex is a rare example of an N_3-coordinated metal–flavin complex is discussed in detail. The dependence of $^{2}J(^{15}N–^{31}P)$ on steric and electronic effects in phosphine and phosphite Au^{I}(ptm) complexes is discussed. The sensitivity of ^{15}N for NMR detection was significantly improved through the use of a $\{^{31}P\}^{15}N$ INEPT pulse sequence. Linear P–Au–N coordination in the bridged complex $Au_2(\mu\text{-}Et_2P(CH_2)_2PEt_2)(ptm\text{-}^{15}N)_2$ was confirmed by analysis of the second-order $\{^{1}H\}^{31}P$ spectrum. The Au(III) complex *trans*-$[AuBr_2(ptm)(PEt_3)]$ was prepared by an oxidative-addition reaction. This complex readily isomerized to the cis isomer. Reactions of $AuBr_3(PEt_3)$ with ptm-^{15}N were followed by ^{31}P NMR. A major product was the cis isomer. Cis $^{2}J(^{15}N–^{31}P)$ couplings were very small (<0.6 Hz) compared to trans couplings (ca. 55 Hz). A similar dependence was found for the related square-planar complexes $[MCl(ptm)(PPh_3)_2]$, M = Pd(II) or Pt(II). The (imido)gold(I) triethylphosphine complexes were all orally active antiinflammatory agents in the carrageenan-induced rat paw edema assay. Reaction of these complexes with thiols is discussed. The (imido)gold(III) phosphines were not tested on account of their high chemical reactivity.

Introduction

A variety of gold(I) phosphine complexes exhibit oral antiinflammatory activity in animal models.[1] Structure–activity correlations within the series R_3P–Au–SR′ (where SR′ is a sugar thiolate) have revealed optimum activity when R_3P is triethylphosphine, and one of these compounds, auranofin ("Ridaura", Smith Kline & French Laboratories) [(2,3,4,6-tetra-*O*-acetyl-1-thio-β-D-glucopyranosato-*S*)(triethylphosphine)gold(I)], is currently undergoing Phase IV clinical testing.

In the current work we set out to synthesize a new series of (imido)gold(I) triethylphosphine complexes. The chosen imides generally exerted biological activity in their own right, and it was hoped that this would enhance both the oral absorption and the biological activity of the gold complexes. The possibility of preparing an analogous series of (imido)gold(III) phosphine complexes was also investigated. The biological (anticancer) activity of isoelectronic square-planar Pt(II) complexes containing nitrogen ligands is well-known,[2] but relatively little attention has been devoted to the chemistry of either Au(I) or Au(III) complexes containing nitrogen ligands.

Although there was early interest in the activity of Au(III) succinimido complexes against microorganism-induced arthritis in mice,[3,4] recent studies[5] have suggested that these were actually 1:2 Au(I):succinimido complexes analogous to sodium bis(*N*-methylhydantoinato)aurate(I). There are a few other reports of gold complexes containing nitrogen ligands,[6] but Au(I)–N bonds especially are considered to be relatively weak.

We also report a study of $^{2}J(^{31}P–^{15}N)$ couplings in a series of ^{15}N-enriched $[Au(ptm\text{-}^{15}N)(PR_3)]$ complexes. Our aim was to investigate the transmission of steric and electronic effects across P–Au–N linkages. These have acquired added interest from reports[7,8] of the antitumor activity of auranofin against P388 leukemia and the possibility that gold binding to DNA bases could occur.[9] The involvement of nitrogen ligands in gold binding to proteins has also been suggested.[10]

Experimental Section

Materials. Sodium salts of 5,5-diphenylhydantoin Na(dph) and saccharin Na(sac) were purchased from Sigma Chemical Co. Ltd., potassium phthalimide K(ptm), riboflavin (ribH), and 3a,4,5,6-tetrahydrosuccinimido[3,4-*b*]acenaphthen-10-one (thsaH) were purchased from Aldrich Chemical Co., Inc., and potassium phthalimide (98% ^{15}N) was purchased from Prochem BOC Ltd.

All phosphines were purchased from Aldrich, except for 1,2-bis(diethylphosphino)ethane (depe) and 1,2-bis(diphenylphosphino)ethane (dppe) from Strem Chemicals. *trans*-$[PdCl_2(PPh_3)_2]$ and *cis*-$[PtCl_2(PPh_3)_2]$ were obtained from Johnson Matthey Ltd.

Experimental Methods. The complexes R_3PAuCl, where R_3P = Et_3P, Ph_3P, $i\text{-}Pr_3P$, $PhEt_2P$, Ph_2EtP, Me_3P, $(OMe)_3P$, or $(OPh)_3P$, and $ClAu(\mu\text{-depe})AuCl$, were prepared as previously described.[11,12]

The gold(III) complex $AuBr_3(PEt_3)$ was prepared by oxidation of Et_3PAuBr as previously described[13] and had a satisfactory elemental analysis and melting point.

Preparation of $Et_3PAu(ptm)$. To a cooled, stirred solution of Et_3PAuCl (0.200 g, 0.57 mmol) in EtOH (10 mL) was added dropwise a solution of potassium phthalimide (0.159 g, 0.86 mmol) in H_2O (3 mL). The solution was stirred for 1 h, and the product was obtained by precipitation with H_2O (ca. 30 mL). This was filtered off and recrystallized from EtOH (5 mL) with the addition of H_2O.

The yield of white needles, mp 113–114 °C, was 0.22 g (82%). Anal. Calcd for $C_{14}H_{19}AuNO_2P$: C, 36.46; H, 4.15; N, 3.04. Found: C, 36.43; H, 4.16; N, 3.16. Crystals suitable for X-ray analysis were obtained by slow evaporation of a solution in $EtOH/H_2O$.

The complex was also prepared in good yield by adding a solution of Et_3PAuCl (0.57 mmol) in EtOH (10 mL) to one of phthalimide (0.86 mmol) in H_2O (3 mL) containing 1 molar equiv of NaOH. From either

† Birkbeck College.
‡ King's College. Present address: CRC Biomolecular Structure Unit, Block F, Clifton Avenue, Sutton, Surrey SM2 5PX, U.K.
§ Smith Kline & French Laboratories.

(1) Sutton, B. M.; McGusty, E.; Walz, D. T.; DiMartino, M. J. *J. Med. Chem.* **1972**, *15*, 1095.
(2) Rosenberg, B. *Met. Ions Biol. Syst.* **1980**, *11*, 127.
(3) Kharasch, M. S.; Isbell, H. S. *J. Am. Chem. Soc.* **1931**, *53*, 3053.
(4) Block, S. D.; Buchanan, O. H.; Freyberg, R. J. *J. Pharmacol. Exp. Ther.* **1944**, *82*, 391.
(5) Malik, N. A.; Sadler, P. J.; Neidle, S.; Taylor, G. L. *J. Chem. Soc., Chem. Commun.* **1978**, 711.
(6) Puddephatt, R. J. "The Chemistry of Gold"; Elsevier: Amsterdam, 1978.
(7) Simon, T. M.; Kunishima, D. H.; Vilbert, G. J.; Lorber, A. *Cancer Res.* **1981**, *41*, 94.
(8) Mirabelli, C. K.; Johnson, R. K.; Sung, C. M.; Faucette, L.; Muirhead, K.; Crooke, S. T. *Cancer Res.* **1985**, *45*, 32.
(9) Blank, C. E.; Dabrowiak, J. C. *J. Inorg. Biochem.* **1984**, *21*, 21.
(10) Otiko, G.; Sadler, P. J. *FEBS Lett.* **1980**, *116*, 227.
(11) McGusty, E. R.; Sutton, B. M. U.S. Patent 3,718,679, Feb 1973.
(12) Berners Price, S. J.; Mazid, M. A.; Sadler, P. J. *J. Chem. Soc., Dalton Trans.* **1984**, 969.
(13) Mann, F. G.; Purdie, D. *J. Chem. Soc.* **1940**, 1235.

0020-1669/85/1324-3425$01.50/0

of these methods, $Et_3PAu(dph)$, $Et_3PAu(sac)$, $Et_3PAu(thsa)$, and $Ph_3PAu(ptm)$ were also prepared in good yield from the appropriate R_3PAuCl complex. All gave satisfactory elemental analyses.

Preparation of $Et_3PAu(rib)\cdot H_2O$. Riboflavin (0.354 g, 0.94 mmol) was dissolved in a solution of NaOH in H_2O (0.038 g, 0.94 mmol in 5 mL). Solid Et_3PAuCl (0.300 g, 0.86 mmol) was immediately added and the mixture shaken vigorously for 5 min. The orange product precipitated from solution and was filtered off, washed with H_2O, acetone, and Et_2O, and dried in vacuo: yield 0.560 g (90%); mp 200 °C. Anal. Calcd for $C_{23}H_{34}AuN_4O_6P\cdot H_2O$: C, 38.99; H, 5.12; N, 7.94; P, 4.37. Found: C, 38.75; H, 4.84; N, 7.91; P, 4.46.

An attempted preparation of the complex by the same method as for $Et_3PAu(ptm)$ gave a mixture of products as evidenced by ^{31}P NMR. This was presumably due, at least in part, to the conversion of riboflavin to lumiflavin after prolonged exposure to alkaline conditions.[14]

Preparation of (ptm)Au(μ-depe)Au(ptm). $[(AuCl)_2(depe)]$ (0.030 g, 0.045 mmol) was dissolved in dimethylformamide (1.5 mL), and K[ptm] (0.018 g, 0.098 mmol) in H_2O (0.5 mL) was added. The clear solution was stirred for 30 min and then freeze-dried. The resulting product was washed thoroughly with H_2O (2 × 2 mL) and dried in vacuo; mp 207–217 °C. Anal. Calcd for $C_{26}H_{32}AuN_2O_4P_2$: C, 34.99; H, 3.61; N, 3.14; P, 6.94. Found: C, 34.72; H, 3.70; N, 3.35; P, 7.27.

Preparation of *trans*-[$AuBr_2$(ptm)(PEt_3)]. $Et_3PAu(ptm)$ (0.20 g, 0.43 mmol) was dissolved in $CHCl_3$ (5 mL) and the solution cooled to 0 °C in a N_2 atmosphere. Br_2 (0.067 g, 21 μL, 0.40 mmol) in $CHCl_3$ (2 mL) was added dropwise, and the resulting yellow solution was stirred for 5 min. The solution was then transferred to a basin, and the solvent was evaporated to dryness under a fume hood. The pale yellow solid was washed with ice-cold Et_2O and dried in vacuo. Anal. Calcd for $C_{14}H_{19}AuBr_2NO_2P$: C, 27.08; H, 3.08; N, 2.25; Br, 25.73; P, 4.99. Found: C, 27.82; H, 3.13; N, 2.17; Br, 23.67; P, 5.14.

The yellow solid usually turned green within a few days when stored either in the dark or light, at 0 or 25 °C, in the presence of air. After several months in these conditions, the solid eventually turned brown.

Preparation of ^{15}N-Enriched Complexes. $Ph_3PAu(ptm\text{-}^{15}N)$ and $Et_3PAu(ptm\text{-}^{15}N)$ were prepared in ca. 85% yield by methods analogous to those used to prepare the nonenriched complexes: addition of 1.1 molar equiv of K[ptm-^{15}N] to a solution of the R_3PAuCl complex. Similarly ^{15}N-labeled (ptm)Au(μ-depe)Au(ptm) was prepared by the addition of 2.2 molar equiv of K[ptm-^{15}N] to $[(AuCl)_2(depe)]$.

$R_3PAu(ptm\text{-}^{15}N)$ complexes, where R_3P = *i*-Pr_3P, $PhEt_2P$, Ph_2EtP, Me_3P, $(OMe)_3P$, or $(OPh)_3P$, were prepared in solution only, by the addition of 1 molar equiv of K[ptm-^{15}N] in H_2O (0.2 mL) to a ca. 65 mM solution of the appropriate R_3PAuCl complexes in either acetone or dimethylformamide. $\{^1H\}^{31}P$ NMR spectra were then recorded at 243 K with acetone-d_6 (0.5 mL) as solvent.

Pd(II) and Pt(II) Phthalimide Complexes. Aliquots of a stock solution of triethylammonium phthalimidate in acetone (prepared in situ from Et_3N and phthalimide) were added to *ca.* 25 mM solutions of either *trans*-$[PdCl_2(PPh_3)_2]$ or *cis*-$[PtCl_2(PPh_3)_2]$ in $CDCl_3$, and ^{31}P NMR spectra were recorded. The same procedure was followed when phthalimide-^{15}N was used.

Reaction of $Et_3PAu(dph)$ and $Et_3PAu(rib)$ with *N*-Acetylcysteine. When either complex was added to a 24 mM solution of *N*-acetylcysteine in D_2O, the solid dissolved within a few minutes as the free imido ligand precipitated. ^{31}P NMR spectra were recorded after adjusting the pH (meter reading) of the supernatant to 7. In both cases a single resonance was observed at 41.0 ppm.

Antiinflammatory Activity. This was measured for the five Et_3PAu(imido) complexes by using the carrageenan rat paw edema assay as previously described.[15] Doses of drug equivalent to between 10–20 mg of Au/kg of body weight were administered orally to male Charles River Lewis or Wistar rats, 1 h before subplantar injection of carrageenan into the right hind paw. The paw volume was determined after 3 h.

NMR Measurements. ^{1}H NMR spectra at 199.5 and 400.13 MHz were recorded on JEOL FX200 and Bruker WH 400 spectrometers, respectively, and were referenced to Me_4Si. $\{^1H\}^{31}P$ NMR spectra were recorded on JEOL FX60 (24.15 MHz) or Bruker HFX 90 (36.4 MHz) machines in 10-mm tubes. H_3PO_4/D_2O (85:15 v/v) was used as an external shift reference.

^{15}N NMR spectra were recorded either by normal (single-pulse) acquisition at 20.3 MHz on a Varian XL200 instrument or at 30.4 MHz on a Bruker AM300 instrument using a $\{^{31}P\}^{15}N$ INEPT (insensitive nuclei enhancement via polarization transfer) pulse sequence:

$$[90°_x(^{31}P)-\tau-[180°_x(^{31}P),180°_x(^{15}N)]-\tau-[90°_y(^{31}P),90°_x(^{15}N)]-\text{FID}$$

with $\tau = {}^1/_4[^2J(^{15}N-^{31}P)]$.

Full experimental details for the ^{31}P-INEPT experiment have been described previously.[16] The ^{15}N shift reference was external $^{15}NH_4SO_4$ (2.9 M in 1 M HCl). In all cases the high-frequency–positive-sign convention is used.

X-ray Absorption Spectra. These were recorded at the SERC Daresbury Laboratory with radiation from the SRS storage ring operating at 2 GeV (150–200 mA). Solid compounds were diluted with boron nitride and mounted between Mylar or Sellotape windows.

Crystal Structure Determination. The crystal employed for the X-ray diffraction study had the dimensions 0.12 × 0.14 × 0.24 mm. Unit cell parameters were determined from Weissenberg photographs and were subsequently refined on an Enraf-Nonius CAD4 automated diffractometer using 25 reflections. The intensity data were measured with Cu Kα radiation[17] (graphite monochromator) on the diffractometer, operated in the ω–2θ scan mode up to θ = 60° ($\pm h,k,l$; h(max) = 12, k(max) = 12, l(max) = 14). Equivalent reflections were averaged (agreement factor 0.030). A periodic check on intensities of three strong reflections showed that no crystal decay occurred during the data collection. Systematic absences [(hkl), $h + k = 2n + 1$; ($0kl$), $l = 2n + 1$; ($0k0$), $k = 2n + 1$] indicated that the space group is either $Pc2_1n$ (No. 33) or $Pcmn$ (No. 62). Both were tried and the former was confirmed. The crystals are noncentrosymmetric, but although both enantiomers were tried, no distinction between them could be made in the refinement.

Crystal Data: $AuC_{14}H_{19}NO_2P$, fw 461.25, orthorhombic, a = 11.004 (1) Å, b = 11.023 (1) Å, c = 12.687 (2) Å, V = 1538.9 Å^3, d_{calcd} = 1.991 g cm^{-3}, d_{measd} = 1.99 g cm^{-3}, Z = 4, F(000) = 880, space group $Pc2_1n$, Cu Kα radiation (λ = 1.5418 Å), μ(Cu Kα) = 192.1 cm^{-1}.

The crystal structure was solved by the heavy-atom method and refined on F by full-matrix least-squares procedures. Out of the 1144 unique reflections observed, 916 with $I > 1.5\sigma(I)$ were used for the refinement. The atomic scattering factors for the non-hydrogen and hydrogen atoms were taken from ref 18 and 19, respectively. Anomalous dispersion corrections from ref 18 were applied to gold and phosphorus atoms. Absorption correction was made by initially using a PSI scan and then by using a program written by Walker and Stuart.[20] Due to the dominant scattering power of gold atoms, it was difficult to refine the parameters of light atoms, and some saturated and unsaturated C–C distances became as long as 1.75 and 1.52 Å, respectively. Therefore refinements were carried out with constraint on C–C, C–O, and C–N bond lengths with an estimated error of 0.01 Å. Only the gold and phosphorus atoms were refined with anisotropic thermal factors. Unit weight was assigned to each reflection. Hydrogen atoms could not be located from a difference Fourier map. The final R factor was 0.045.

Table I. Unit Cell Positional and Thermal Parameters for $Et_3PAu(ptm)$ with Estimated Standard Deviations in Parentheses

atom	x	y	z	U_{iso}/U_{eq},[a] Å^2
Au	−0.1538 (1)	0	−0.1452 (1)	0.0345 (5)
P	−0.3320 (6)	0.001 (2)	−0.0603 (5)	0.036 (3)
O_1	0.041 (2)	0.207 (2)	−0.225 (2)	0.035 (6)
O_2	0.034 (2)	−0.207 (2)	−0.259 (2)	0.049 (7)
N	0.009 (1)	−0.001 (4)	−0.223 (1)	0.039 (5)
C_1	−0.464 (2)	0.014 (5)	−0.146 (2)	0.041 (6)
C_2	−0.587 (2)	0.021 (4)	−0.090 (2)	0.053 (8)
C_3	−0.351 (2)	−0.119 (2)	0.030 (2)	0.021 (6)
C_4	−0.238 (3)	−0.156 (3)	0.094 (3)	0.033 (8)
C_5	−0.363 (3)	0.157 (3)	0.010 (3)	0.041 (9)
C_6	−0.257 (4)	0.196 (5)	0.081 (4)	0.09 (2)
C_7	0.074 (4)	0.104 (3)	−0.245 (4)	0.05 (2)
C_8	0.185 (3)	0.066 (3)	−0.305 (3)	0.02 (1)
C_9	0.286 (3)	0.119 (4)	−0.354 (4)	0.06 (1)
C_{10}	0.379 (3)	0.049 (3)	−0.398 (3)	0.05 (1)
C_{11}	0.376 (3)	−0.077 (3)	−0.394 (3)	0.05 (1)
C_{12}	0.279 (2)	−0.134 (3)	−0.345 (3)	0.026 (8)
C_{13}	0.185 (4)	−0.060 (4)	−0.310 (5)	0.06 (2)
C_{14}	0.069 (4)	−0.102 (3)	−0.262 (4)	0.02 (1)

[a] $U_{eq} = (U_1U_2U_3)^{1/3}$ for Au and P.

(14) Yagi, K. *Methods Biochem. Anal.* **1962**, *10*, 319.
(15) Walz, D. T.; DiMartino, M. J.; Griffin, C. L.; Misher, A. *Arch. Int. Pharmacodyn. Ther.* **1970**, *185*, 337.
(16) Brevard, C.; Shimpf, R. *J. Magn. Reson.* **1982**, *47*, 528.
(17) Mo Kα radiation would have been preferable, but was not available to us.
(18) "International Tables for X-ray Crystallography"; Kynoch Press: Birmingham, England, 1974; Vol. IV.
(19) Stewart, R. F.; Davidson, E. R.; Simpson, W. T. *J. Chem. Phys.* **1965**, *42*, 3175.
(20) Walker, N.; Stuart, D. *Acta Crystallogr., Sect. A: Found. Crystallogr.* **1983**, *A34*, 158.

Table II. Bond Lengths (Å) and Angles (deg) with Estimated Standard Deviations in Parentheses

Au–P	2.238 (6)	C_7–O_1	1.22 (1)
Au–N	2.05 (2)	C_7–C_8	1.49 (1)
P–C_1	1.83 (2)	C_8–C_9	1.39 (1)
P–C_3	1.76 (3)	C_8–C_{13}	1.39 (1)
P–C_5	1.97 (4)	C_9–C_{10}	1.39 (1)
C_1–C_2	1.54 (1)	C_{10}–C_{11}	1.39 (1)
C_3–C_4	1.53 (1)	C_{11}–C_{12}	1.40 (1)
C_5–C_6	1.53 (1)	C_{12}–C_{13}	1.39 (1)
N–C_7	1.40 (1)	C_{13}–C_{14}	1.49 (1)
N–C_{14}	1.39 (1)	C_{14}–O_2	1.22 (1)
N–Au–P	179.8 (5)	N–C_7–C_8	107 (2)
Au–P–C_1	114.2 (7)	C_7–C_8–C_9	139 (3)
Au–P–C_3	114 (1)	C_7–C_8–C_{13}	108 (3)
Au–P–C_5	112 (1)	C_9–C_8–C_{13}	113 (4)
C_1–P–C_3	111 (2)	C_8–C_9–C_{10}	122 (3)
C_1–P–C_5	94 (2)	C_9–C_{10}–C_{11}	121 (4)
C_3–P–C_5	109 (1)	C_{10}–C_{11}–C_{12}	119 (4)
P–C_1–C_2	115 (2)	C_{11}–C_{12}–C_{13}	116 (3)
P–C_3–C_4	117 (2)	C_{12}–C_{13}–C_8	127 (4)
P–C_5–C_6	113 (3)	C_{12}–C_{13}–C_{14}	125 (3)
Au–N–C_7	123 (3)	C_8–C_{13}–C_{14}	107 (3)
Au–N–C_{14}	126 (3)	C_{13}–C_{14}–N	108 (2)
C_7–N–C_{14}	110 (1)	C_{13}–C_{14}–O_2	126 (4)
N–C_7–C_8	107 (2)	N–C_{14}–O_2	127 (4)
O_1–C_7–C_8	128 (4)		

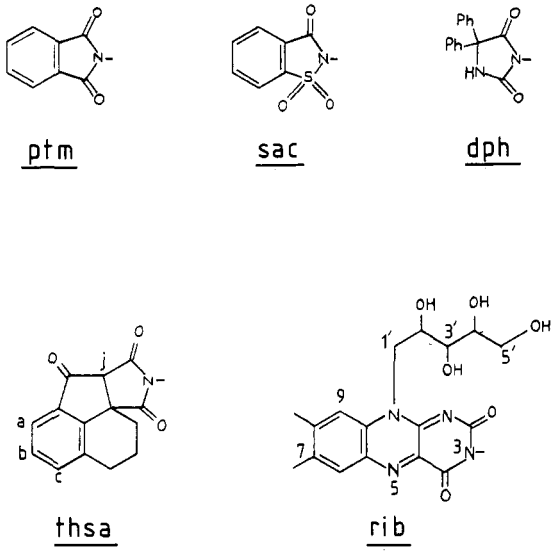

Figure 1. Structures of the imido ligands.

The highest residual electron density was 0.81 $e/Å^3$. All the calculations were carried out on PDP 11/34A and CDC 7600 computers with the SDP crystallographic program system[21] and SHELX.[22] The atomic coordinates and bond lengths and angles are listed in Tables I and II, respectively.

Results

Preparation and Characterization of R_3PAuN(imide) Complexes. Air-stable, white or cream-colored complexes of general formula $Et_3PAu(NR')$ were prepared in good yield from Et_3PAuCl for the imido ligands phthalimide (ptm), 5,5-diphenylhydantoin (dph), saccharin (sac), and 3a,4,5,6-tetrahydrosuccinimido[3,4-*b*]acenapthen-10-one (thsa) (Figure 1). The analogous riboflavin complex could not be prepared by the same method, as prolonged reaction under alkaline conditions led to mixed products, presumably as a result of hydrolysis of the ribityl side chain. However,

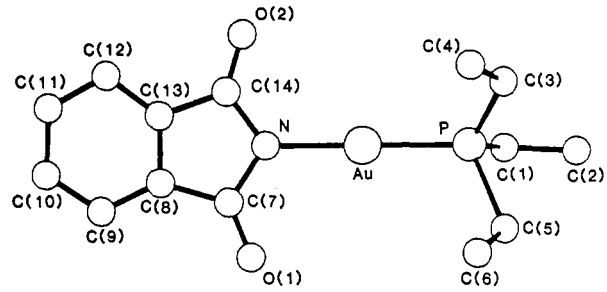

Figure 2. Molecular structure of Et_3PAu(ptm) showing the numbering system.

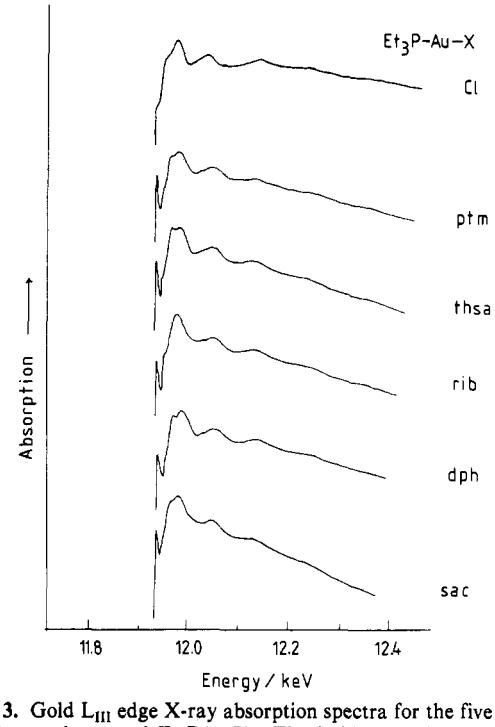

Figure 3. Gold L_{III} edge X-ray absorption spectra for the five Et_3PAu(imido) complexes and Et_3PAuCl. The imido complexes all show a characteristic sharp spike at ca. 11.92 keV.

the orange complex Et_3PAu(rib) was prepared quantitatively, by dissolving Et_3PAuCl in an aqueous solution of riboflavin at pH 10. All these complexes had satisfactory elemental analyses and were further characterized by ^1H NMR. Selected physical data are shown in Table III.

^1H NMR spectra of each of the five Et_3PAu(imide) complexes contained a doublet of triplets and a doublet of quartets for the PCH_3 and PCH_2 protons, and integration of the spectra confirmed a 1:1 Et_3PAu:imide stoichiometry in each case. The phthalimide protons of Et_3PAu(ptm) were shielded with respect to those of the free ligand, and a similar upfield coordination shift was observed for the aromatic protons of thsa (Table IV). The cyclohexane protons of this ligand were not individually assigned, but a range of coordination shifts is evident. Linear coordination in Et_3PAu(ptm) was confirmed by the crystal structure shown in Figure 2. The N–Au–P angle is 180°, and Au–N and Au–P bond lengths are 2.05 and 2.24 Å, respectively. Bond distances and interbond angles are listed in Table II.

Gold L_{III} edge X-ray absorption spectra provided evidence that all the E_3PAu(imido) complexes have similar P–Au–N coordination in the solid state. These are shown in Figure 3. Each shows a characteristic sharp line in the XANES region near 11.92 keV, which is not observed for Et_3PAuCl.

The Riboflavin Complex. Riboflavin contains a number of possible N-binding sites.[23] The UV absorption spectrum of

(21) Frenz, B. A. "Enraf-Nonius Structure Determination Packages"; Enraf-Nonius: Delft, Holland, 1980.
(22) Sheldrick, G. M. "SHELX 76", A system of computer programs for X-ray crystallography; University of Cambridge: Cambridge, England, 1976.
(23) Hemmerich, P.; Lauterwein, J. In "Inorganic Biochemistry"; Eichorn, G. L., Ed.; Elsevier: Amsterdam, 1973; Vol. 2, 1168–90.

Table III. Selected Physical and Spectroscopic Data for Au(I) and Au(III) Phosphine Imido Complexes

complex	mp, °C	^{1}H NMR,[a] δ				^{31}P NMR[b]	
		CH_3[c]	CH_2[d]	phenyl	other	δ	$^2J(^{31}P-^{15}N)$,[e] Hz
Et_3PAu(ptm)	113–114	1.26	1.92	7.68[f]		29.6	41
Et_3PAu(dph)	245–248	1.22	1.88	7.33, 7.46	5.7 (NH)	28.9	
Et_3PAu(sac)	148–150	1.26	1.93	7.70, 7.86		30.0	
Et_3PAu(thsa)	215	1.18	1.82	*g*	*g*	29.3	
Et_3PAu(rib)	200	1.18[h]	1.95[h]	*i*	*i*	32.9[j]	
Ph_3PAu(ptm)	200–205			7.67[f], 7.54		32.7	43
(ptm)Au(μ-depe)Au(ptm)	207–217	1.32	2.06	7.64[f]	2.24[k] (CH_2)	30.3	39
trans-[$AuBr_2$(ptm)(PEt_3)]	124–127	1.37	2.53	7.62[f]		35.4	57

[a] Relative to Me_4Si, solvent $CDCl_3$. [b] Relative to external 85% H_3PO_4, solvent $CDCl_3$. [c] Doublet of triplets. $^3J(^{31}P-^1H)$ = 18–19 Hz; $^3J(^1H-^1H)$ = 7.5 Hz. [d] Doublet of quartets. $^2J(^{31}P-^1H)$ = 10–11 Hz; $^3J(^1H-^1H)$ = 7.5 Hz. [e] Probably has a negative sign. [f] Phthalimide protons analyzed as an AA'BB' spin system. [g] Complete ^{1}H NMR data listed in Table IV. [h] In Me_2SO. [i] Ribityl and isoalloxazine protons are indicated in Figure 5. [j] Solvent 3:1 Me_2SO/EtOH with D_2O external lock. [k] Broad singlet for bridge CH_2 protons; $^2J(^{31}P-^1H)$ coupling not resolved.

Table IV. 200-MHz ^{1}H NMR Data for thsaH and Et_3PAu(thsa) in $CDCl_3$

compd	δ values							
	aromatic protons			cyclohexane protons[a]	other			
	H_a[c]	H_b[d]	H_c[c]		H_j	NH	PCH_3[e]	PCH_2[f]
thsaH	7.67	7.50	7.57	3.36–1.70	3.68	7.92		
Et_3PAu(thsa)	7.61	7.38	7.50	3.40–2.41[b]	3.56		1.18	1.82

[a] These occurred as a series of overlapping second-order multiplets and were not individually assigned. [b] Integration indicates that two of the cyclohexane protons are obscured by the PCH_2 protons. [c] Doublet. $^3J(^1H-^1H)$ = 7 Hz. [d] Triplet. $^3J(^1H-^1H)$ = 7 Hz. [e] Doublet of triplets. $^3J(^{31}P-^1H)$ = 18.5 Hz; $^3J(^1H-^1H)$ = 7.5 Hz. [f] Doublet of quartets. $^2J(^{31}P-^1H)$ = 11 Hz; $^2J(^1H-^1H)$ = 7.5 Hz.

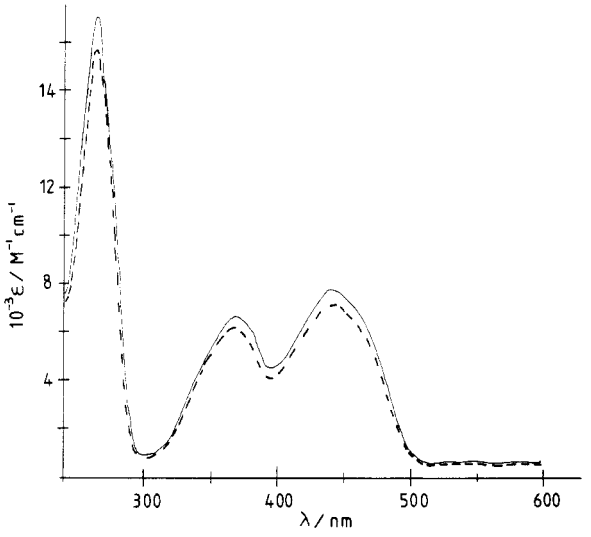

Figure 4. Comparison of the electronic absorption spectra of riboflavin (—) and Et_3PAu(rib) (- -) (8.5×10^{-5} M in 0.1 M phosphate buffer, pH 7).

Et_3PAu(rib) is shown in Figure 4. The gold complex has absorption bands virtually identical with riboflavin alone, consistent with complexation at the N_3 nitrogen atom.[24]

The ^{1}H NMR spectrum of Et_3PAu(rib) in Me_2SO is shown in Figure 5B. The absence of a resonance for the N_3 proton is again consistent with gold binding at this site. However, this proton (pK_a = 10)[25] would have been ionized under the alkaline reaction conditions. In order to further investigate the binding site, the ^{1}H NMR spectrum of free riboflavin was recorded at the same concentration and temperature (Figure 5A), and the coordination shift for each proton was determined. The assignments for the ^{1}H NMR resonances of free riboflavin in Me_2SO have not been previously reported and were made with the aid of selective homonuclear decoupling experiments.

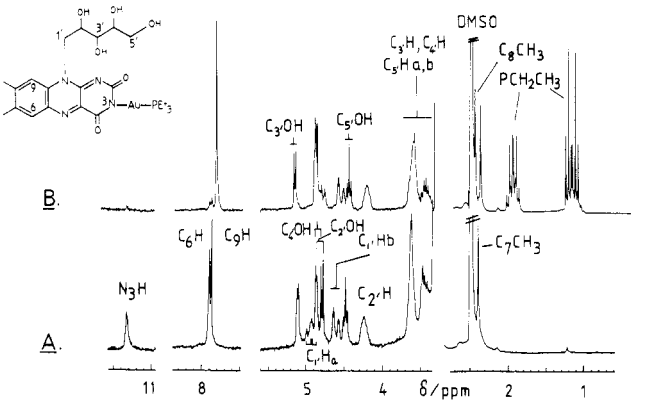

Figure 5. 200-MHz ^{1}H NMR spectra of 5.6 mM solutions of (A) riboflavin and (B) Et_3PAu(rib) in Me_2SO at 300 K. The disappearance of the resonance for the N_3H proton and the small coordination shifts for the ribityl and isoalloxazine protons are apparent; see text.

The two C_1' protons are nonequivalent and give rise to doublet of doublet resonances at 4.95 [$J(1'a-1'b)$ = 12 Hz, $J(1'a-2')$ = 9 Hz)] and 4.61 ppm [$J(1'a-1'b)$ = 12 Hz, $J(1'b-2')$ = 2 Hz].[26] The respective $J(1'-2')$ coupling constants indicate that the $C_1'a$ proton is trans to $C_2'H$ and $C_1'b$ is gauche, in agreement with observations of Kainosho and Kyogoku.[27]

The C_2' proton gives a broad resonance at 4.25 ppm, which sharpens on irradiation of either C_1' proton. The $C_3'C_4'$ and C_5' protons cannot be individually assigned by selective decoupling, due to overlapping resonances, but these gave rise to the unresolved multiplets at 3.64 and 3.48 ppm. Irradiation of the $C_5'OH$ proton indicates the two C_5' protons are nonequivalent.

The isoalloxazine protons were assigned with reference to previous ^{1}H NMR studies of flavoquinone molecules,[28-30] for which

(24) It has been reported that chelation at the N_5–O_4 site causes a red shift and protonation or alkylation at N_1 results in a blue shift, whereas deprotonation or complexation at N_3 does not significantly shift the position of the flavine absorption bands. See ref 23.
(25) Heelis, P. F. *Chem. Soc. Rev.* **1982**, *11* (1), 15–39.
(26) A large chemical shift difference between C_1' protons has also been reported for FMN and FAD in D_2O and was attributed to the fact that one of the rotational isomers around the glycosidic bond is populated exclusively, so that $C_1'H_a$ is located close to the N_1 atom, whereas $C_1'H_b$ resides at the aryl side of the isoalloxazine ring (see ref 27). This is observed in the solid state: Voet, D.; Rich, A. *Proc. Natl. Acad. Sci. U.S.A.* **1971**, *68*, 1151.
(27) Kainosho, M.; Kyogoku, Y. *Biochemistry* **1972**, *11*, 741–52.
(28) Lauterwein, J.; Hemmerich, P.; Lhoste, J. M. *Inorg. Chem.* **1975**, *14*, 215.
(29) Bullock, F. J.; Jardetzky, O. *J. Org. Chem.* **1965**, *30*, 2056.

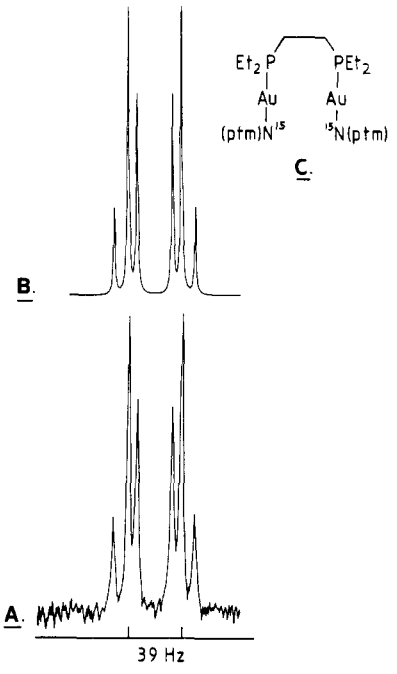

Figure 6. (A) Observed and (B) simulated $\{^1H\}^{31}P$ NMR spectrum at 36.4 MHz of the ^{15}N-enriched binuclear complex shown in part C. The multiplet pattern was analyzed as an AA'XX' spin system.

the relative shieldings increase in the order $H_{(6)} < H_{(9)} < CH_{3(8)} < CH_{3(7)}$, independent of the solvent.[31]

Only the $C_2'OH$ and $C_5'OH$ hydroxyl protons could be unambiguously assigned by selective decoupling. The C_3' and C_4' hydroxyl protons account for the doublets at 5.10 and 4.85 ppm, and it seems likely that the least shielded resonance is due to $C_3'OH$ since this is closer to the isoalloxazine ring.

The isoalloxazine ring and ribityl protons of $Et_3PAu(rib)$ (Figure 5B) are all shifted to low frequency with respect to free riboflavin in the order $C_1'Ha$ (0.15) > C_6H (0.09) > C_9H (0.07) > $C_1'Hb$ (0.05) > $C_2'H$ (0.04) > C_8CH_3 (0.03) > C_7CH_3 (0.02), where the figures in parentheses are the chemical shift differences in ppm. The two spectra were recorded under identical conditions, and so the observed shifts are not merely a result of temperature or concentration effects. Furthermore, ionization of the N_3 proton of riboflavin by the addition of NaOD caused only a very slight upfield shift of the isoalloxazine resonances by between 0.01 and 0.02 ppm. The observed coordination shifts must therefore be a result of gold binding.

The magnitude of the C_6H and C_9H coordination shifts indicates that binding cannot be to the N_5–O_4 site, for which coordination shifts of between 0.2 and 0.5 ppm might be expected.[28] The coordination shifts for the ribityl C_1' protons are too small for complexation to be at the N_1 nitrogen atom but are of a size comparable to those arising from complexation at N_5. The relative order of all the coordination shifts is fully consistent with N_3 coordination. The greater perturbation of the $C_1'a$ proton with respect to $C_1'b$ fits in with the proposal of Kainosho and Kyogoku[26,27] that the $C_1'a$ proton resides close to the N_1 nitrogen atom, whereas $C_1'Hb$ is located near the aromatic isoalloxazine ring.

ptm-^{15}N Complexes. All complexes containing phthalimide ligands were further characterized by recording the ^{31}P NMR spectra of the ^{15}N isotopically enriched compounds. Both $Et_3PAu(ptm\text{-}^{15}N)$ and $Ph_3PAu(ptm\text{-}^{15}N)$ gave well-resolved doublet resonances with $^2J(^{31}P\text{–}^{15}N)$ couplings of 41 and 43 Hz, respectively.[32] This provides unequivocal evidence that P–Au–N coordination persists in solution. The ^1H NMR spectra were identical with those of the nonenriched complexes. $^4J(^1H\text{–}^{15}N)$ couplings were not observed.

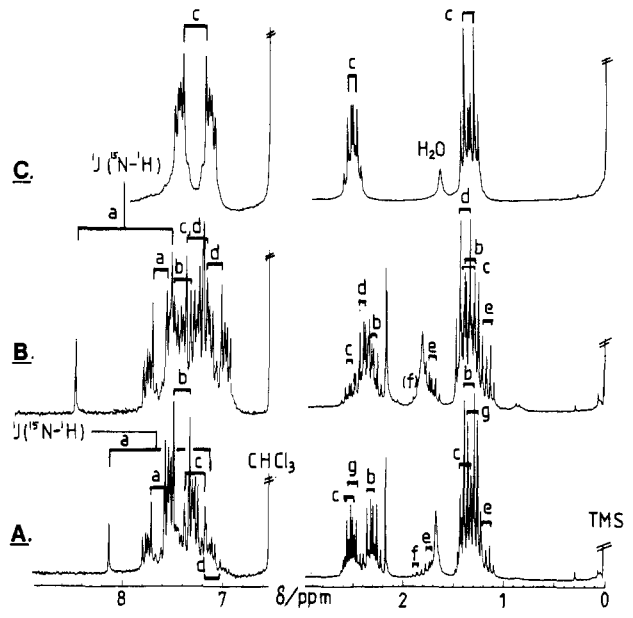

Figure 7. 200-MHz ^1H NMR spectra of products from the reaction of $AuBr_3(PEt_3)$ with (A) 1 molar equiv of K[ptm] and (B) 2 molar equiv of K[ptm]. For each product the PCH_3, PCH_2 and phthalimide multiplets are labeled in the manner shown in part C for *trans*-$[AuBr_2(ptm)(PEt_3)]$. The assignments are as follows: a, ptmH; b, *cis*-$[AuBr_2(ptm)(PEt_3)]$; c, *trans*-$[AuBr_2(ptm)(PEt_3)]$; d, *cis*-$[AuBr(ptm)_2(PEt_3)]$; e, Et_3PO; f, Et_3PAuBr; g, $[AuBr_3(PEt_3)]$. The Et_3PAuBr PCH_3 resonance is obscured by the Et_3PO PCH_3 resonance.

The binuclear complex (ptm)Au(μ-depe)Au(ptm) (Figure 6C) exhibited only a single $\{^1H\}^{31}P$ NMR resonance as a result of the magnetic equivalence of the two phosphorus atoms. However, with incorporation of two spin-$^1/_2$ ^{15}N nuclei into the complex, the spin system becomes second order.

The $\{^1H\}^{31}P$ spectrum of the ^{15}N-enriched complex at 300 K consists of a six-line multiplet pattern (Figure 6A). This was analyzed according to the rules of Günther,[33] as the AA' part of an AA'XX' spin system in which $J(XX') = 0$ Hz. The derived $^2J(^{31}P\text{–}^{15}N)$, $^3J(^{31}P\text{–}^{31}P)$ and $^5J(^{31}P\text{–}^{15}N)$ coupling constants of −39.1, 16.9, and 0.1 Hz, respectively were used to simulate the spectrum shown in Figure 6B, which is an exact fit to the experimental spectrum. The analogous complex (ptm)Au(μ-dppe)Au(ptm) was prepared in situ and was not isolated. The $\{^1H\}^{31}P$ NMR spectrum of a solution in DMF/H_2O (3:1 v/v) gave only a single resonance at ambient temperature, but this resolved into a six-line AA'XX' multiplet at 240 K. The following coupling constants were obtained by the same procedure: $^2J(^{31}P\text{–}^{15}N) = -40.4$ Hz, $^3J(^{31}P\text{–}^{31}P) = 25.0$ Hz, $^5J(^{31}P\text{–}^{15}N) = 0.1$ Hz.

$^2J(^{31}P\text{–}^{15}N)$ couplings were also observed by ^{15}N NMR. The isotopically enriched complex $Et_3PAu(ptm\text{-}^{15}N)$ gave a doublet resonance at 179.5 ppm, with $^2J(^{31}P\text{–}^{15}N) = 41$ Hz. However, due to the low sensitivity and long relaxation time of the ^{15}N nucleus, a spectrum with a good signal to noise ratio required about 12 h of experiment time for a 0.1 M solution.

We have recently demonstrated[34] that in cases where $^{31}P\text{–}^{109}Ag$ couplings are resolved, the application of a $\{^{31}P\}^{109}Ag$ INEPT pulse sequence results in considerable savings in experiment time for the observation of the insensitive ^{109}Ag nucleus. By the use of an analogous $\{^{31}P\}^{15}N$ INEPT pulse sequence the ^{15}N NMR spectrum of $Et_3PAu(ptm\text{-}^{15}N)$ was obtained. A 1:1 "up down" doublet at 179.5 ppm characteristic of an AX spin system was resolved after only 4 repetitions of the pulse sequence for a 50

(30) Sarma, R. H.; Dannies, P.; Kaplan, N. O. *Biochemistry* **1968**, *7*, 435.
(31) For FAD the chemical shifts of the H_6 and H_9 resonances may be reversed at high concentrations. This has been attributed to interactions between the flavin and adenine rings (ref 27).
(32) A well-resolved doublet, $J = 41$ Hz, was also seen in the solid-state ^{15}N NMR spectrum of $Et_3PAu(ptm\text{-}^{15}N)$: Morden, K.; Opella, S.; Berners Price, S. J.; Sadler, P. J., unpublished.
(33) Günther, H. *Angew. Chem.* **1972**, *11*, 861.
(34) Berners Price, S. J.; Sadler, P. J.; Brevard, C.; Pagelot, A. *Inorg. Chem.*, in press.

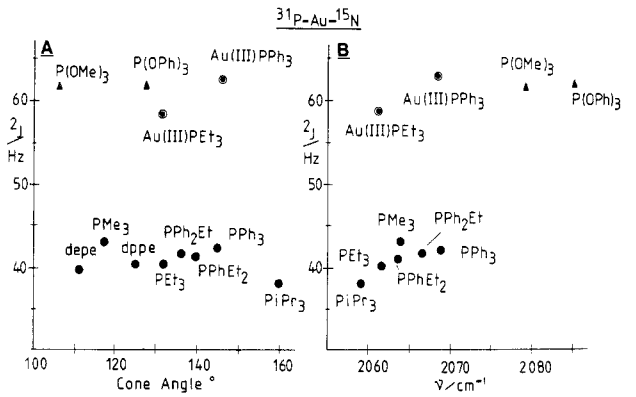

Figure 8. Plots of $^2J(^{31}P-^{15}N)$ couplings in $R_3PAu(ptm-^{15}N)$ phosphine (●) and phosphite (▲) complexes vs. (A) cone angle (θ) and (B) the electronic parameter (ν) (see text). The points labeled Au(III) refer to the complexes of type *trans*-$[AuBr_2(ptm)(PR_3)]$.

mM solution of the isotopically enriched complex. ^{15}N NMR spectra were also recorded for $Et_3PAu(ptm)$ at natural abundance level by using the $\{^{31}P\}^{15}N$ INEPT method. A spectrum with a reasonable signal to noise ratio was obtained after ca. 5 h from a 0.5 M solution.

In order to investigate the dependence of $^2J(^{31}P-^{15}N)$ couplings on the nature of the phosphine ligand, a series of $R_3PAu(ptm-^{15}N)$ complexes were prepared in situ from the appropriate R_3PAuCl complex. $\{^1H\}^{31}P$ NMR spectra were all recorded at 243 K, because in some cases $^2J(^{31}P-^{15}N)$ couplings were not resolved at room temperature. Complexes of arylphosphines were found to be more kinetically labile than those of alkylphosphines, for which couplings were always resolved at 300 K. As can be seen in Figure 8, the $^2J(^{31}P-^{15}N)$ couplings for $R_3PAu(ptm)$ complexes containing phosphine ligands, 38–43 Hz, are lower than those of phosphite complexes, 61 Hz, or gold(III) phosphines, 57 Hz (vide infra).

Au(III) Complexes: Oxidation of $Et_3PAu(ptm)$. Careful oxidation of $Et_3PAu(ptm)$ with Br_2 in $CHCl_3$ produced a yellow solid, which had an elemental analysis consistent with the formulation $[AuBr_2(ptm)(PEt_3)]$. The complex gave a single $\{^1H\}^{31}P$ NMR resonance at 35.4 ppm, which split into a doublet $[^2J(^{31}P-^{15}N) = 57$ Hz] when ^{15}N-enriched $Et_3PAu(ptm-^{15}N)$ was used.

The ^1H NMR spectrum is shown in Figure 7C. The PCH_2 and PCH_3 multiplet resonances are substantially deshielded with respect to those for the Au(I) complex but have chemical shifts typical of gold(III) phosphines.[35] The phthalimide protons occur as a characteristic AA'BB' multiplet with a larger low-field coordination shift than that of the Au(I) complex.

The magnitude of the $^2J(^{31}P-^{15}N)$ coupling constant is similar to the trans $^2J(^{31}P-^{15}N)$ coupling observed in related d^8 Pt(II) and Pd(II) complexes (vide infra) and suggests that *trans*-$[AuBr_2(ptm)(PEt_3)]$ exclusively is formed by oxidation of $Et_3PAu(ptm)$. However, ^{31}P NMR spectra of reaction solutions containing ^{15}N-enriched starting material revealed that if a slight excess of Br_2 was added, or reaction times were prolonged, then mixed products were formed. By comparison with the ^{31}P NMR spectra of the authentic complexes, minor peaks at 34.2 and 47.6 ppm were identified as Et_3PAuBr and $AuBr_3(PEt_3)$. The latter assignment was confirmed by the increase in intensity of the 47.6 ppm resonance with increasing addition of Br_2. A very minor doublet resonance at 41.5 ppm, $^2J(^{31}P-^{15}N) = 55$ Hz, was assigned to the bis(phthalimido) complex *cis*-$[AuBr(ptm)_2(PEt_3)]$, which was the major substitution product from the reaction of $AuBr_3(PEt_3)$ with excess phthalimide (vide infra). This product could have resulted from the presence of trace amounts of free phthalimide in the starting material but was more likely a product of redox equilibrium 1, which would also account for the formation of Et_3PAuBr.[36]

(35) Cf. $AuBr_3(PEt_3)$: δCH_3, 1.34; CH_2, 2.54.

$$[AuBr_2(ptm)(PEt_3)] + Et_3PAu(ptm) \rightleftharpoons [AuBr(ptm)_2(PEt_3)] + Et_3PAuBr \quad (1)$$

After longer reaction times a more intense singlet resonance appeared at 52.2 ppm. Since no $^2J(^{31}P-^{15}N)$ coupling was resolved and cis $^2J(^{31}P-^{15}N)$ couplings are often very small in magnitude,[37,38] the resonance was tentatively assigned to *cis*-$[AuBr_2(ptm)(PEt_3)]$.

To investigate further the possibility that isomerization of *trans*-$[AuBr_2(ptm)(PEt_3)]$ may occur to form the thermodynamically stable cis isomer, substitution reactions of $AuBr_3(PEt_3)$ with phthalimide were investigated.

Reaction of $AuBr_3(PEt_3)$ with ptm-^{15}N. An orange solid was isolated from the reaction of $AuBr_3(PEt_3)$ (30 mM in chloroform) with 1 molar equiv of $K[ptm-^{15}N]$ (75 mM in methanol) after evaporation of the solvent. ^{31}P and ^1H NMR spectra of this product, when redissolved in $CDCl_3$, both revealed that this consisted of six distinct species. The $\{^1H\}^{31}P$ NMR spectrum had resonances at 52.4, 48.1, 35.4 $[^2J(^{31}P-^{15}N) = 57$ Hz], 52.9, 41.8 $[^2J(^{31}P-^{15}N) = 55$ Hz], and 34.3 ppm, listed in order of decreasing intensity. The ^1H NMR spectrum is shown in Figure 7A, and consists of overlapping multiplets for the PCH_3, PCH_2, and phthalimide protons of the individual species. These occur as a doublet of triplets $[^3J(^{31}P-^1H) \simeq 19$ Hz], a doublet of quartets $[^2J(^{31}P-^1H) \simeq 10$ Hz] and AA'BB' multiplets respectively. By comparison with the ^{31}P NMR spectra of the authentic species the resonances at 48.1, 52.9, and 34.3 ppm can be assigned to $AuBr_3(PEt_3)$, Et_3PO, and Et_3PAuBr. Multiplet PCH_3 and PCH_2 NMR resonances attributable to these species are also observed.[39] The relative intensities of these ^1H NMR multiplets are in agreement with those of the corresponding ^{31}P resonances.

A small amount of *trans*-$[AuBr_2(ptm)(PEt_3)]$ was identified from both the ^{31}P (35.4 ppm) and ^1H NMR spectra and the other minor ^{31}P resonance, which showed a trans $^2J(^{31}P-^{15}N)$ coupling, was assigned to *cis*-$[AuBr(ptm)_2(PEt_3)]$.

The major product of the reaction has a singlet ^{31}P NMR resonance at 52.4 ppm, and the major ^1H NMR multiplets occur at 1.34 (PCH_3), 2.31 (PCH_2), and 7.70 ppm (phthalimide). Since $^2J(^{31}P-^{15}N)$ coupling is not resolved, but phthalimide ^1H NMR resonances are observed, this provides very strong evidence that *cis*-$[AuBr_2(ptm)(PEt_3)]$ is the major product of this substitution reaction. The ^{31}P NMR chemical shift is in agreement with the previous assignment for the cis isomer formed by isomerization of *trans*-$[AuBr_2(ptm)(PEt_3)]$ (vide supra).

A yellow solid was isolated from the reaction of $AuBr_3(PEt_3)$ (15 mM in chloroform) with 2 molar equiv of $K[ptm-^{15}N]$ (75 mM in MeOH], after evaporation of the solvent. The ^1H NMR spectrum of this solid, redissolved in $CDCl_3$, is shown in Figure 7B. The major multiplets at 1.39 (PCH_3), 2.39 (PCH_2), and 7.56 and 7.63 (phthalimide) ppm are assigned to the bis(phthalimido) complex *cis*-$[AuBr(ptm)_2(PEt_3)]$, and, in accord with this assignment, the major resonance in the ^{31}P NMR spectrum is now the doublet $[^2J(^{31}P-^{15}N) = 55$ Hz] at 41.8 ppm. This has increased in intensity at the expense of both *cis*-$[AuBr_2(ptm)(PEt_3)]$, which is now the second most abundant species, and to a lesser extent *trans*-$[AuBr_2(ptm)(PEt_3)]$. There are no ^1H or ^{31}P NMR resonances assignable to $AuBr_3(PEt_3)$, but Et_3PAuBr and Et_3PO are again observed. It is noteworthy that both of the ^1H NMR spectra show intense AA'BB' multiplets at 7.80 ppm due to free, protonated phthalimide $[^1J(^{15}N-^1H) = 95$ Hz].

Stability of *trans*-$[AuBr_2(ptm)(PEt_3)]$. This yellow complex is not stable in air for long periods. The solid usually becomes

(36) A similar scheme has been proposed to account for the mixed $[AuCl_nBr_{3-n}PR_3]$ complexes formed by oxidation of R_3PAuCl with Br_2: (a) Puddephatt, R. J.; Thompson, P. J. *J. Chem. Soc., Dalton Trans.* **1975**, 1810. (b) Heaton, B. T.; Kelsey, R. J. *Inorg. Nucl. Chem. Lett.* **1975**, *11*, 363.

(37) Carty, A. J. *Inorg. Chem.* **1976**, *15*, 1956.

(38) Carty, A. J.; Jacobson, S. E. *J. Chem. Soc., Chem. Commun.* **1975**, 175.

(39) Et_3PAuBr and Et_3PO are also produced when $AuBr_3(PEt_3)$ alone is dissolved in chloroform/methanol, and there have been other reports that significant amounts of Au(I) are produced after a time from solutions of $AuX_3(PEt_3)$ (X = halide) (see ref 36b).

Scheme I

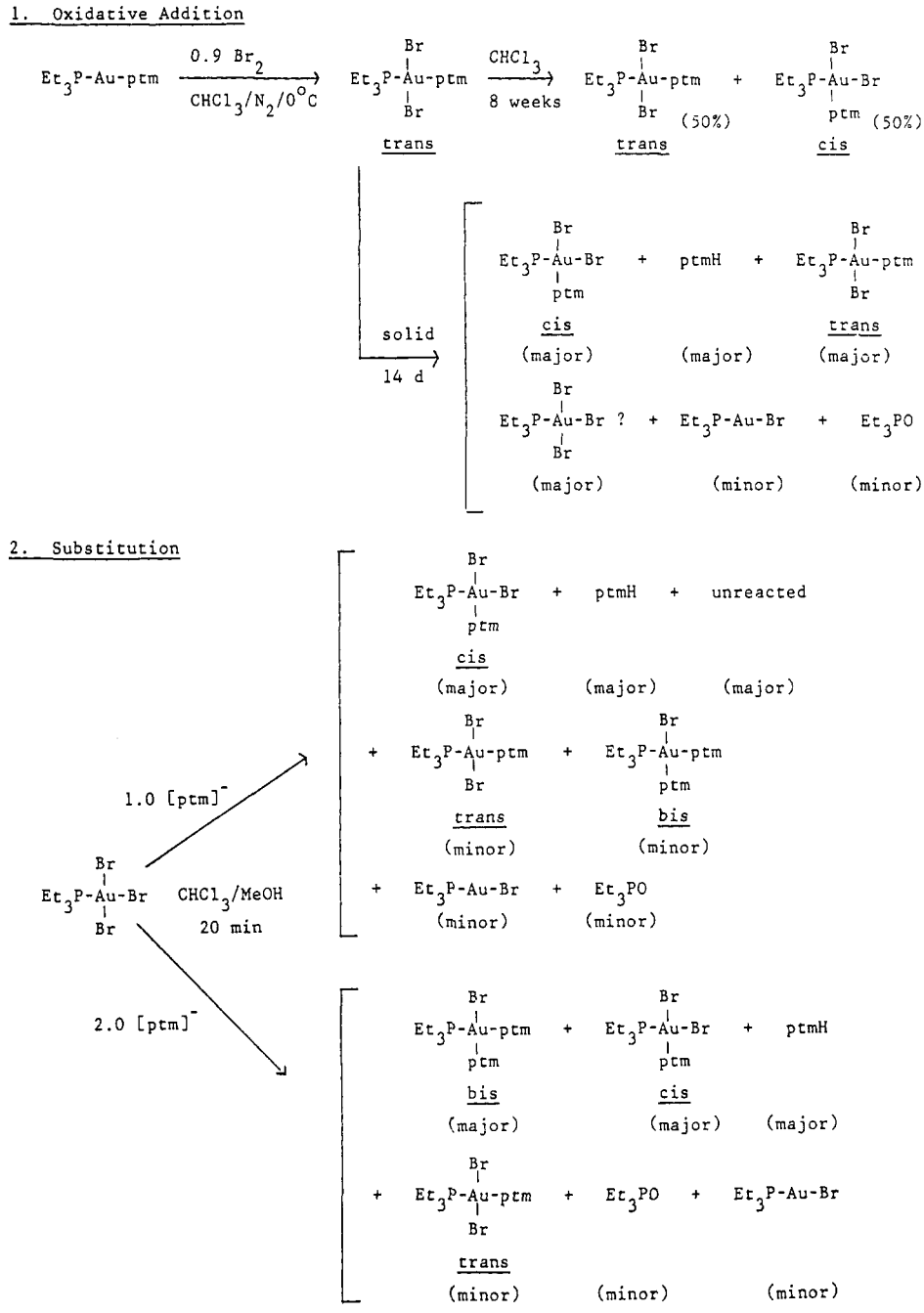

green within a few days, even in the dark at 0 °C.

The ^{1}H NMR spectrum of the green solid showed major multiplet resonances for free, protonated phthalimide (7.82 ppm) *cis*-[$AuBr_2$(ptm)(PEt_3)] (δ: CH_3, 1.34; CH_2, 2.31; ptm, 7.70) and $AuBr_3(PEt_3)$ (δ: CH_3; 1.31; CH_2, 2.51). Minor multiplet resonances with the correct chemical shifts for Et_3PAuBr and Et_3PO were also observed, but *trans*-[$AuBr_2$(ptm)(PEt_3)] was only a minor component of the mixture. After several months of storage at 300 or 273 K, the brown solid contained only a trace amount of the trans isomer and there were now no ^{1}H NMR resonances assignable to *cis*-[$AuBr_2$(ptm)(PEt_3)]. The ^{31}P NMR spectrum consisted of four peaks at 51.6, 52.2, 56.7, and 71.4 ppm together with an intense resonance at 47.4 ppm. This was assigned to $AuBr_3(PEt_3)$, for which ^{1}H NMR multiplets are also found. The remaining four sets of ethyl resonances in the ^{1}H NMR spectrum could not be assigned, but a very intense AA'BB' multiplet for free phthalimide was observed.

A solution of *trans*-[$AuBr_2$(ptm-^{15}N)(PEt_3)] in $CDCl_3$ that was left for two months remained yellow, whereas a similar sample of the solid stored in a sample tube for the same time became green. The ^{1}H NMR spectrum of the yellow solution showed only two sets of multiplets, of approximately equal intensity, for *trans*- and *cis*-[$AuBr_2$(ptm)(PEt_3)]. No other decomposition had occurred.

Our observations on reactions involving (imido)gold(III) phosphine complexes are summarized in Scheme I.

$^2J(^{31}P-^{15}N)$ Couplings in Pt(II) and Pd(II) Complexes. The ^{31}P NMR studies of $AuBr_2$(ptm-^{15}N)(PEt_3) indicated that cis $^2J(^{31}P-^{15}N)$ couplings for gold(III) complexes are very small (<0.6 Hz) compared to trans couplings (ca. 55 Hz). Reactions of the related square-planar d^8 complexes *cis*-[$PtCl_2(PPh_3)_2$] and *trans*-[$PdCl_2(PPh_3)_2$] with phthalimide-^{15}N were followed by ^{31}P NMR spectroscopy to confirm this pattern of cis and trans $^2J(^{31}P-^{15}N)$ couplings.

The ^{31}P NMR spectrum of *cis*-[$PtCl_2(PPh_3)_2$] consisted of a singlet resonance at 13.6 ppm with associated ^{195}Pt satellites. On addition of increasing amounts of phthalimide (Et_3NH^+ salt) to the solution, this resonance was replaced by two doublet resonances [$^2J(^{31}P-^{31}P)$ = 18 Hz] at 14.2 and 7.4 ppm, together with ^{195}Pt satellites. When [Et_3NH](ptm-^{15}N) was used, the low field

Table V. Antiinflammatory Activity of (Triethylphosphine)gold(I) Imide Complexes

imide	oral dose[a]	% inhibition[b]
phthalimide (I)	15	42**
diphenylhydantoin (II)	10	36*
saccharin (III)	20	38**
riboflavin (IV)	20	65**
(tetrahydrosuccinimido)-acenaphthenone (V)	20	50**
auranofin	5	17*
	10	24**
	20	56**

[a] In mg Au/kg. [b] Percent inhibition of paw volume increase in the rat carrageenan assay. A single asterisk denotes $P < 0.05$ and a double asterisk denotes $P < 0.01$ as significant differences from control with use of Student's t test. Results are based on 7–8 rats per test group and 12 rats in control groups.

doublet remained unchanged, whereas the 7.4 ppm doublet, (together with the appropriate ^{195}Pt satellites) showed additional $^2J(^{31}P–^{15}N)$ coupling of 51 Hz.

The observation of $^2J(^{31}P–^{31}P)$ couplings establishes that the two ^{31}P resonances correspond to nonequivalent phosphine groups in the same complex and allows unequivocal identification of the product as *cis*-$[PtCl(ptm)(PPh_3)_2]$. The trans $^2J(^{31}P–^{15}N)$ coupling is 51 Hz, whereas the cis coupling must be <0.6 Hz, since no further splitting of the 14.2 ppm doublet was resolved. The larger $^1J(^{195}Pt–^{31}P)$ coupling (3842 Hz) is associated with the least shielded phosphine ligand (trans to Cl^-). The ligand trans to phthalimide has a $^1J(^{195}Pt–^{31}P)$ value of 3168 Hz. This reflects the higher trans influence of the phthalimide ligand. The $^1J(^{195}Pt–^{31}P)$ couplings occur within the expected range.[40]

No further change in the ^{31}P NMR spectrum was observed when up to 4 molar equiv of phthalimide were added, and so substitution of the second Cl^- ligand by phthalimide does not readily occur.

On addition of $[Et_3NH]$ptm to a solution of *trans*-$[PdCl_2(PPh_3)_2]$, the singlet ^{31}P NMR resonance at 22.8 ppm diminished in intensity at the expense of two doublet resonances [$^2J(^{31}P–^{31}P)$ = 9 Hz] at 34.2 and 25.2 ppm. These may be assigned to the nonequivalent phosphine ligands in *cis*-$[PdCl(ptm)(PPh_3)_2]$. Cis stereochemistry was confirmed by repeating the titration with ptm-^{15}N. Both doublets split into four lines as a result of $^2J(^{31}P–^{15}N)$ coupling. A cis $^2J(^{31}P–^{15}N)$ coupling of 2 Hz was just resolved for the low-field resonance, which can be unambiguously assigned to PPh_3 trans to Cl^-. The 25.2 ppm resonance showed a large trans $^2J(^{31}P–^{15}N)$ coupling of 51 Hz.

A minor singlet resonance was also observed at 21.4 ppm. This increased in intensity at the expense of the peak for *trans*-$[PdCl_2(PPh_3)_2]$. Since no $^2J(^{31}P–^{31}P)$ coupling was resolved and the resonance occurred to slightly higher field of that of the starting material, the most likely assignment is *trans*-$[PdCl(ptm)(PPh_3)_2]$ in which both PPh_3 ligands are equivalent, and trans to one another. However, no cis $^2J(^{31}P–^{15}N)$ coupling was resolved, and so this assignment could not be confirmed.

Antiinflammatory Activity of Et_3PAu(imido) Complexes. All five complexes were effective in inhibiting the increase in hind paw volume in the rat carrageenan assay (Table V), and the activity of the riboflavin complex is comparable to that of auranofin at the same oral gold dose. In view of the instability of the gold(III) phosphine imido complexes, they were not tested for activity.

Discussion

Structure of Et_3PAu(imido) Complexes. Gold(I) complexes containing N-ligands are relatively rare and are generally stable only when a strong π-acceptor ligand is also coordinated to gold. Thus tertiary phosphine complexes of type R_3PAuNR', where NR' = pyridine,[41] imidazole,[42] and bipyridyl,[43] are all stable complexes whereas chloro(piperidine)gold(I) rapidly disproportionates in air.[44] Malik and co-workers[5] have reported the structure of a stable bis(*N*-methylhydantoinato)gold(I) complex in which Au(I) is coordinated to N-ligands only, and in this case the N-ligands themselves are able to participate in back-bonding via the carbonyl π orbitals.

The N-ligands reported here share the 1,3-dicarbonylimido structure of *N*-methylhydantoin, and the stability of the $R_3P–Au–$(*N*-imido) complexes is thus a reflection of the strong π-acceptor properties of both the phosphine and imido ligands.

The Au–N bond distance (2.05 Å) in Et_3PAu(ptm) is comparable to that in chloro(piperidine)gold(I) (2.07 Å)[44] and shorter than either Au–N bond in $(bpy)(PPh_3)Au$[43] (2.41, 2.17 Å). The increased Au–N bond distance with respect to bis(*N*-methylhydantoinato)gold(I) (1.94 Å),[5] presumably reflects the high trans influence of PEt_3. The Au–P bond distance is similar to that of the gold(I) phosphine thiolate complex auranofin[45] (2.29 Å). Strong evidence that all five Et_3PAu(imido) complexes have similar P–Au–N coordination is provided by their X-ray absorption spectra taken at the L_{III} gold edge (Figure 3). Each complex gives a characteristic sharp spike in the near-edge region. We have observed a similar feature for gold(I) phosphine complexes with two or more phosphine ligands, and the intensity of the spike increases with the number of bound phosphines.[46] Elder and co-workers have observed a similar trend.[47] Since Au(I) has a filled 5d shell it seems likely that the spike arises from an electronic transition from gold 2p orbitals to a molecular orbital involving vacant π-acceptor orbitals of the imido ligands. It is not observed for Et_3PAuCl. This type of metal–ligand interaction is also indicated by the ^1H NMR spectra of the complexes, where the imido protons are generally shielded with respect to those of the free ligands.[48] This observation is of special interest for the riboflavin complex, since it has previously been reported that binding of a diamagnetic ion, e.g. Ag^+, to the N_5 nitrogen atom generally causes a downfield shift of the protons of the isoalloxazine ring.[28] The observed shielding of these protons in Et_3PAu(rib) is consistent with Au(I) binding to the N_3 nitrogen atom and with back-donation of d electrons from the metal into the vacant π orbitals of the ligand. In view of our previous work on Au(I)–hydantoinato complexes,[5] N_3 coordination in Et_3PAu(rib) is not totally unexpected since this is also part of a 1,3-dicarbonylimido system. However, N_3 is not a commonly observed binding site in metal–flavin complexes.[23] Metal–flavin complexes have been classified into different types according to the polarizability of the metal ion. The less polarizable ions such as Mg^{2+} and Fe^{3+} form only monodentate complexes with very weak binding to the carbonyl oxygen atoms. Under anhydrous conditions a variety of more polarizable ions form so-called "flavoquinone chelate complexes" involving chelation at the $N_5–O_4$ site. These generally hydrolyze on removal of the N_3 proton under aqueous conditions. Exceedingly soft metal ions such as Ag(I) and Cu(I) form $N_5–O_4$ "charge-transfer chelates" under alkaline conditions.

Two crystallographic studies of complexes of riboflavin with $AgClO_4$[49a] and $Cu(ClO_4)_2$[49b] have confirmed a primary $N_5–O_4$ binding site for these metal ions, and secondary binding sites were found at N_1, O_2, and $O_{2'}$ and O_2, $O_{4'}$, and $O_{5'}$, respectively. These

(40) Pregosin, P. S.; Kunz, R. W. "^{31}P and ^{13}C NMR of Transition Metal Phosphine Complexes"; Springer-Verlag: West Berlin, 1979.
(41) Hill, D. T., European Patent 3,897, 1979.
(42) Bonati, F.; Felici, M.; Pietroni, B. R.; Burini, A. *Gazz. Chim. Ital.* **1982**, *112*, 5.
(43) Clegg, W. *Acta Crystallogr., Sect. B: Struct. Crystallogr. Cryst. Chem.* **1976**, *B32*, 2712.
(44) Guy, J. J.; Jones, P. G.; Mays, M. J.; Sheldrick, G. M. *J. Chem. Soc., Dalton Trans.* **1977**, 8.
(45) Hill, D. T.; Sutton, B. M. *Cryst. Struct. Commun.* **1980**, *9*, 679.
(46) Berners Price, S. J.; Ismail, I. M.; Mazid, M. A.; Razi, M. T.; Sadler, P. J.; Greaves, G. N., "Proceedings of a Conference on Biological Systems: Structure and Analysis, March 1984"; SERC: Daresbury, U.K.; DL/SC1/R22, p 18.
(47) Elder, R. C.; Eidsness, M. J.; Heeg, M. J.; Tepperman, K. G.; Shaw, C. F., III; Shaeffer, N. *ACS Symp. Ser.* **1983**, *No. 209*, 385.
(48) A similar deshielding of imido ^1H NMR resonances has recently been reported for N-bonded Ag(I)–succinimido complexes: Perron, J.; Beauchamp, A. L. *Inorg. Chem.* **1984**, *23*, 2853.
(49) (a) Wade, T. D.; Fritchie, C. J. *J. Biol. Chem.* **1973**, 248, 2337–2343. (b) Garland, W. T.; Fritchie, C. J. *J. Biol. Chem.* **1974**, *249*, 2228.

complexes were prepared under either acidic or neutral conditions and in both cases the N_3 atom was protonated. Gold(I) coordination at N_3 underlines the marked preference of Au(I) for linear, two-coordination, whereas the other d^{10} ions Ag(I) and Cu(I) more often form tetrahedral complexes.

Gold(III) Phosphine Imido Complexes. Gold(III) does not share with gold(I) the requirement for stabilization by "soft" donor ligands, and several Au(III) complexes with nitrogen ligands are known.[6] These include a few complexes with imido ligands. Tyabi and Gibson[50] reported the preparation of saccharin and phthalimido complexes of type $K[AuX_2(imido)_2]$ (X = Cl, Br) and a succinimido complex $K[Au(suc)_3Br]$. They were unable to isolate the tetrasuccinimido–Au(III) complex reported by Kharasch and Isbell,[3] and Malik and co-workers[5] have suggested that this complex was probably a 1:2 Au(I) complex analogous to sodium bis(*N*-methylhydantoinato)gold(I).

By oxidation of $Et_3PAu(ptm)$ with bromine, we have prepared $[AuBr_2(ptm)(PEt_3)]$. Trans stereochemistry was established by the large (55 Hz) $^2J(^{31}P-^{15}N)$ coupling. Oxidative-addition reactions of $[Au(C_6X_5)(PEt_3)]$[51] and $[Au(CN)_2]^-$[52] with halogen have also been shown to give similar trans products.

Ligand substitution reactions of gold(III) complexes are always very much faster (ca. $\times 10^4$)[53] than for Pt(II) complexes and have not been investigated in nearly so much detail. Kinetic studies have mainly been concerned with the entry of amines into, or displacement from, chlorogold complexes,[6] and recent investigations have included the displacement by chloride of the nitrogen–oxygen chelate pyridine-2-carboxylate from $[AuCl_2(N-O)]$.[54]

It is usually assumed that the mechanism of the substitution reactions involves a five-coordinate transition state, and this has been identified in the reaction of $[AuCl_4]^-$ with SCN^-.[55] Isolation of stable complexes such as $[AuCl(P\text{-}P)_2]^{2+}$, where P-P is 1,2-bis(dimethylphosphino)benzene,[56] and $[AuCl_3(2,2'\text{-biquinolyl})]$[57] have indicated that five-coordinate gold(III) shows a preference for square-pyramidal stereochemistry.

The very much faster substitution of chloride by pyridine in $AuCl_3(PPh_3)$ than in $[AuCl_4]^-$ or $AuCl_3(py)$ suggests that PPh_3 exerts a high trans effect.[58] The crystal structure of the complex revealed a longer Au–Cl distance for the chlorine trans to phosphine and a significant distortion from square-planar stereochemistry, so that the high reactivity may be a result of both a weakening of the ground-state Au–Cl bond, and a stabilization of the five-coordinate transition state.[58]

In the light of these observations, it may be predicted that substitution of halide (X) by a ligand Y in AuX_3PR_3 will take place by an associative mechanism with retention of configuration giving *trans*-$[AuX_2(Y)PR_3]$. The reaction of $AuBr_3(PEt_3)$ with phthalimide gave a mixture of products including *trans*-$[AuBr_2(ptm)(PEt_3)]$, but ^1H and ^{31}P NMR spectra provided strong evidence that the cis isomer was the major product. Isomerization of the pure trans complex occurred both in solution and in the solid state, suggesting that the cis isomer is the more thermodynamically stable product.

Isomerization reactions of d^8-metal complexes have been reviewed[59] and are common in Pt(II) chemistry. However, observation of cis–trans isomerization in gold(III) chemistry has been reported only for the organogold(III) complexes *trans*-$[AuCl_2(C_6Br_5)(PPh_3)]$[60] and *trans*-$[AuMe_2Et(PPh_3)]$.[61] A mechanism involving dissociation of PPh_3 and rearrangement of a 3-coordinate T-shaped intermediate was proposed.

Further investigation of the substitution and isomerization reactions of the gold(III) phthalimido complexes was hampered by the high reactivity of the products. *trans*-$[AuBr_2(ptm)PEt_3)]$ slowly isomerized in chloroform solution, but when stored in air, it also underwent decomposition with release of phthalimide. $AuBr_3(PEt_3)$ was identified as the major product, although bromine-bridged dimeric or oligomeric complexes would be expected to have similar ^1H and ^{31}P NMR spectra.

Measurement and Significance of $^2J(^{31}P-^{15}N)$ Coupling Constants. ^{31}P chemical shifts often show little dependence on the nature of the trans ligand in R_3PAuY complexes. For instance, all of the $Et_3PAu(imido)$ complexes studied here have ^{31}P NMR resonances between 28 and 33 ppm, which is close to the shift of Et_3PAuCl (31.4 ppm). The ^{31}P NMR resonances were generally slightly broadened ($\Delta\nu_{1/2} \simeq 15$ Hz) at 302 K, presumably as a result of coupling to the quadrupolar ^{14}N ($I = 1$) nucleus. When a solution of $Et_3PAu(ptm)$ was heated in DMF to 356 K, the ^{31}P NMR resonance broadened further ($\Delta\nu_{1/2} = 30$ Hz), consistent with the expected behavior for a spin-$^1/_2$ nucleus coupled to a quadrupolar nucleus, but $^{31}P-^{14}N$ spin–spin coupling was not resolved. This result is expected since the ^{14}N nucleus does not exist in an environment of high electrical symmetry, and so the rate of ^{14}N relaxation will be rapid. The only reported example of resolved $^{14}N-^{31}P$ coupling in a coordination complex is for the Pt(II)–isothiocyanate complex *cis*-$Pt(NCS)(SCN)(P(OPh)_3)_2$, and similar coupling was not resolved at ambient temperature for the analogous Pd(II) complex.[38]

In this study the potential of ^{31}P NMR spectroscopy for detecting P–M–N linkages was greatly increased by the use of isotopically enriched ligands and the observation of two-bond $^2J(^{31}P-^{15}N)$ couplings. This technique proved particularly useful for characterization of the binuclear complexes $(ptm)Au(\mu\text{-}P\text{-}P)Au(ptm)$ where P-P is dppe or depe. The observation of second-order AA'XX' $\{^1H\}^{31}P$ NMR spectra, confirmed that the structure contained two linear P–Au–N linkages, Figure 6. Analysis of the AA'XX' spectra allowed direct measurement of the three-bond $^{31}P-^{31}P$ coupling constant, which is rarely observed for symmetrical $R_2P(CH_2)_2PR_2$ ligands.[62]

For the series of $R_3PAu(ptm\text{-}^{15}N)$ complexes the magnitude of the $^2J(^{31}P-^{15}N)$ coupling is expected to reflect the strength of the P–Au bond. This is usually discussed in terms of both the steric and electronic effects of the different phosphine substituents.[63] In Figure 8B $^2J(^{31}P-^{15}N)$ values are plotted against the electronic parameter (ν) of the R_3P ligands. This is the frequency of the A_1 carbonyl mode of $Ni(CO)_3PR_3$ in CH_2Cl_2 and has been shown by Tolman[63] to be independent of steric factors. Figure 8A shows a plot of $^2J(^{31}P-^{15}N)$ values against the cone angle of each phosphine ligand. Some correlations are apparent in both cases. For instance, increasing the cone angle decreases the s character of the phosphorus lone pair, and a weaker P–M bond is predicted. In our series this will be reflected by a smaller $^2J(^{31}P-^{15}N)$ value, and this trend is observed as the cone angle increases for $Me_3P < Et_3P < i\text{-}Pr_3P$. However, for these alkylphosphines the $^2J(^{31}P-^{15}N)$ value also correlates very well with the electronegativity of the ligands.

For phosphines with phenyl substituents the $^2J(^{31}P-^{15}N)$ value decreases in the order $Ph_3P > Ph_2EtP > Et_2PhP$, and this trend fits in well with the ligand electronic parameters.

It is evident that for both $(OPh)_3P$ and $(OMe)_3P$ the magnitude of $^2J(^{31}P-^{15}N)$ is very much larger than predicted by consideration of only the P–Au bond strength. This presumably reflects the poorer trans influence of the phosphite ligands so that the Au–N

(50) Tyabi, A. M.; Gibson, C. S. *J. Chem. Soc.* **1952**, 450.
(51) Uson, R.; Laguna, A.; Bergareche, B. *J. Organomet. Chem.* **1980**, *184*, 411.
(52) Ford-Smith, M. H.; Habeeb, J. J.; Rawsthorne, J. H. *J. Chem. Soc., Dalton Trans.* **1972**, 2116.
(53) Basolo, F.; Pearson, R. G. "Mechanisms of Inorganic Reactions", 2nd ed.; Wiley: New York, 1967; p 410.
(54) Annibale, G.; Canovese, L.; Cattalini, L.; Marangoni, G.; Michelon, G.; Tobe, M. L. *J. Chem. Soc., Dalton Trans.* **1984**, 1641.
(55) Hall, A. J.; Satchell, D. P. N. *J. Chem. Soc., Chem. Commun.* **1976**, 163.
(56) Warren, L. F.; Bennett, M. A. *Inorg. Chem.* **1976**, *15*, 3126.
(57) Charlton, R. J.; Harris, C. M.; Patil, H.; Stephenson, N. C. *Inorg. Nucl. Chem. Lett.* **1966**, *2*, 409.
(58) Bandoli, G.; Clemente, D. A.; Marangoni, G.; Cattalini, L. *J. Chem. Soc., Dalton Trans.* **1973**, 886.
(59) Anderson, G. K.; Cross, R. J. *Chem. Soc. Rev.* **1980**, *9*, 185.
(60) Uson, R.; Laguna, A. *Synth. React. Inorg. Met.-Org. Chem.* **1975**, *5*, 17.
(61) Komiya, S.; Albright, T. A.; Hoffmann, R.; Kochi, J. K. *J. Am. Chem. Soc.* **1976**, *98*, 7255.
(62) Colquhoun, I. J.; McFarlane, W. *J. Chem. Soc., Dalton Trans.* **1982**, 1915.
(63) Tolman, C. A. *Chem. Rev.* **1977**, *77*, 313.

bonds will be stronger than for the analogous phosphine complexes. A similar trend has been observed for the platinum(II) complexes $[Pt(^{15}NCS)_2(PR_3)_2]$, where trans $^2J(^{31}P-^{15}N)$ couplings are ca. 55 Hz and ca. 90 Hz for phosphine and phosphite ligands, respectively.[37,38] The observation of identical coupling constants for $(PhO)_3PAu(ptm)$ and $(MeO)_3PAu(ptm)$ can be explained by Tolman's argument[63] that the cone angle of a phosphite ligand does not give an accurate representation of the steric bulk, because the oxygen atoms provide enough flexibility for the OPO angles to remain essentially constant.

The trans $^2J(^{31}P-^{15}N)$ coupling in the gold(III) complexes $[AuBr_{3-n}(ptm)_n(PEt_3)]$ (n = 1 or 2; ca. 55 Hz) is larger than for $Et_3PAu(ptm)$, reflecting the increased Au–N bond strength for the higher oxidation state. The related square-planar d^8 Pt(II) and Pd(II) complexes $[M(Cl)(ptm)(PPh_3)_2]$ have comparable trans $^2J(^{31}P-^{15}N)$ coupling constants. Cis $^2J(^{31}P-^{15}N)$ couplings were found to be very much smaller for all the d^8 complexes and, in fact, were resolved only for $[PdCl(ptm)(PPh_3)_2]$. A similar dependence for cis and trans $^2J(^{31}P-^{15}N)$ couplings has been reported for the Pt(II) complexes $[PtCl_2(py\text{-}^{15}N)(PPh_3)]$[64] and $[Pt(^{15}NCS)(SCN)(P(OPh)_3)_2]$.[38]

The observation of two-bond $^{31}P-^{15}N$ couplings by ^{31}P NMR spectroscopy clearly provides a very useful method for identifying the substitution products of metal phosphine complexes with ^{15}N isotopically enriched ligands. We have also utilized the well-resolved scalar couplings for a second purpose and that is to enhance the NMR signals of the insensitive ^{15}N nucleus by transfer of spin polarization from ^{31}P via a $\{^{31}P\}^{15}N$ INEPT pulse sequence.

Using this method, we were largely able to overcome the unfavorable features of ^{15}N NMR, viz. low sensitivity and long spin–lattice relaxation times (T_1). The repetition time of the pulse sequence is governed by the ^{31}P and not the ^{15}N T_1 value, and the theoretical maximum signal enhancement is given by the ratio $\gamma(^{31}P)/\gamma(^{15}N)$, i.e. 4.0. The considerable sensitivity gain of the $\{^{31}P\}^{15}N$ INEPT method was clearly demonstrated by the observation of a ^{15}N NMR resonance for $Et_3PAu(ptm)$ with ^{15}N in natural abundance. A spectrum with a reasonable signal to noise ratio was obtained within a few hours for a 0.5 M solution.

We hope that the range of $^2J(^{31}P-^{15}N)$ couplings obtained in this study for linear R_3P–Au–N(imide) complexes, will serve as a useful model for monitoring the possible interaction of R_3PAu^+ species with other N-donor ligands such as nucleic acid bases and DNA. Although several R_3PAuY compounds exhibit antitumor activity,[65] and auranofin is known to be an effective inhibitor of DNA, RNA, and protein syntheses,[66] there have been few investigations of the DNA binding properties of gold(I) compounds. Blank and Dabrowiak[9] have recently studied the interactions of a series of gold(I) complexes with calf thymus DNA using absorption and circular dichroism spectroscopy. They observed no interaction for auranofin, but Et_3PAuX, where X = Cl^- or Br^-, did bind and showed a preference for guanine and cytosine residues. Hadjiliadas[67] and co-workers have reported isolation of gold(I) complexes of guanosine and inosine, for which they propose binding at the N_7 site.

Our observation of well-resolved $^2J(^{31}P-^{15}N)$ couplings by ^{15}N NMR at natural-abundance level using a $\{^{31}P\}^{15}N$ INEPT method should be of particular value for studying the interaction of R_3PAu^+ with nucleic acid bases. Enhancement of ^{15}N NMR signals by transfer of ^{31}P spin polarization does not require an exact knowledge of the magnitude of the $^2J(^{31}P-^{15}N)$ coupling.[16]

Antiinflammatory Activity. The variations in the observed activities may partially reflect the extent of oral absorption of each complex. However the in vivo displacement of the imido ligand by a naturally occurring thiolate such as glutathione, would be expected to occur very readily. This was demonstrated in vitro by the reactions of $Et_3PAu(rib)$ and $Et_3PAu(dph)$ with *N*-acetylcysteine. Neither complex is significantly soluble in water, but both dissolved in an aqueous solution of the thiolate, with release of the free imido ligand. The product was identified as a 1:1 Et_3PAu–(*N*-acetylcysteine) complex by the ^{31}P NMR chemical shift at 41.0 ppm. This is characteristic for a P–Au–S linkage. For instance, the ^{31}P chemical shift of auranofin in phosphate buffer is 43.4 ppm.[68]

Acknowledgment. We thank Dr. B. M. Sutton (SKF Laboratories) for his interest and encouragement with this work, Dr. C. Brevard (Bruker Spectrospin) for recording the $\{^{31}P\}^{15}N$ INEPT spectrum, and Dr. N. Greaves and the staff of the Daresbury Laboratory for their help in recording EXAFS spectra. We are grateful to Smith Kline & French Laboratories, the Science and Engineering Research Council, the Medical Research Council, and the University of London, Intercollegiate Research Service, for their support.

Registry No. $Et_3PAu(ptm)$, 97825-49-5; $Et_3PAu(dph)$, 97825-50-8; $Et_3PAu(sac)$, 97825-51-9; $Et_3PAu(thsa)$, 97825-52-0; $Et_3PAu(rib)$, 97860-53-2; $Ph_3PAu(ptm)$, 97825-53-1; $(ptm)Au(\mu\text{-}depe)Au(ptm)$, 97825-54-2; *trans*-$[AuBr_2(ptm)(PEt_3)]$, 97825-55-3; Et_3PAuCl, 15529-90-5; $[(AuCl)_2(depe)]$, 83543-39-9; $Ph_3PAu(ptm\text{-}^{15}N)$, 97860-54-3; $Et_3PAu(ptm\text{-}^{15}N)$, 97825-56-4; $(ptm\text{-}^{15}N)Au(\mu\text{-}depe)Au(ptm\text{-}^{15}N)$, 97825-57-5; $(i\text{-}Pr_3P)Au(ptm\text{-}^{15}N)$, 97860-55-4; $(PhEt_2P)Au(ptm\text{-}^{15}N)$, 97825-58-6; $(Ph_2EtP)Au(ptm\text{-}^{15}N)$, 97825-59-7; $(Me_3P)Au(ptm\text{-}^{15}N)$, 97825-60-0; $((OMe)_3P)Au(ptm\text{-}^{15}N)$, 97825-61-1; $((OPh)_3P)Au(ptm\text{-}^{15}N)$, 97860-56-5; $(i\text{-}Pr_3P)AuCl$, 33659-45-9; $(PhEt_2P)AuCl$, 97825-62-2; $(Ph_2EtP)AuCl$, 16569-58-7; $(Me_3P)AuCl$, 15278-97-4; $((OMe)_3P)AuCl$, 33634-99-0; $((OPh)_3P)AuCl$, 14243-62-0; *trans*-$[PdCl_2(PPh_3)_2]$, 28966-81-6; *cis*-$[PtCl_2(PPh_3)_2]$, 15604-36-1; *cis*-$[AuBr(ptm)_2(PEt_3)]$, 97825-63-3; $AuBr_3(PEt_3)$, 56213-25-3; *cis*-$[AuBr_2(ptm)(PEt_3)]$, 97905-44-7; *cis*-$[PtCl(ptm)(PPh_3)_2]$, 97825-64-4; *cis*-$[PdCl(ptm)(PPh_3)_2]$, 97825-65-5; Et_3PAu(*N*-acetylcysteine), 86421-42-3; auranofin, 34031-32-8.

Supplementary Material Available: Tables of elemental analytical data for (imido)gold(I) phosphine complexes and observed and calculated structure factors for $Et_3PAu(ptm)$ (5 pages). Ordering information is given on any current masthead page.

(64) Ismail, I. M.; Green, M.; Sadler, P. J., unpublished.
(65) Sadler, P. J.; Nasr, N.; Narayanan, V. L. In "Platinum Coordination Complexes in Cancer Chemotherapy"; Hacker, M. P., Douple, E. B., Krakhoff, I. H., Eds.; Martinus Nijhoff Publishers: Boston, 1984; pp 290–304.
(66) Simon, T. M.; Kunishima, D. H.; Vibert, G. J.; Lorber, A. *Cancer (Philadelphia)* **1979**, *44*, 1965.
(67) Hadjiliadas, N.; Pneumatitakis, G.; Basosi, R. *J. Inorg. Biochem.* **1981**, *14*, 115.
(68) Razi, M. T.; Sadler, P. J.; Hill, D. T.; Sutton, B. M. *J. Chem. Soc. Dalton Trans.* **1983**, 1331.